AFRL-RV-PS-
TP-2012-0005

IMPROVING DATA DRIVERS FOR CORONAL AND SOLARWIND MODELS (POSTPRINT)

C. Nick Arge, et al.

8 February 2012

Technical Paper

AIR FORCE RESEARCH LABORATORY
Space Vehicles Directorate
3550 Aberdeen Ave SE
AIR FORCE MATERIEL COMMAND
KIRTLAND AIR FORCE BASE, NM 87117-5776

REPORT DOCUMENTATION PAGE

Form Approved
OMB No. 0704-0188

1. REPORT DATE *(DD-MM-YYYY)*	2. REPORT TYPE	3. DATES COVERED *(From - To)*
08-02-2012	Technical Paper	01 Oct 2007 – 18 Jun 2010

4. TITLE AND SUBTITLE

Improving Data Drivers for Coronal and SolarWind Models (Postprint)

5a. CONTRACT NUMBER

5b. GRANT NUMBER

5c. PROGRAM ELEMENT NUMBER
62601F

6. AUTHOR(S)

C. Nick Arge[1], Carl J. Henney[1], Josef Koller[2], W. Alex Toussaint[3], John W. Harvey[3], and Shawn Young[1]

5d. PROJECT NUMBER
1010

5e. TASK NUMBER
PPM00004579

5f. WORK UNIT NUMBER
EF004380

7. PERFORMING ORGANIZATION NAME(S) AND ADDRESS(ES)

Air Force Research Laboratory
Space Vehicles Directorate
3550 Aberdeen Ave. SE
Kirtland AFB, NM 87117-5776

8. PERFORMING ORGANIZATION REPORT NUMBER

AFRL-RV-PS-TP-2012-0005

9. SPONSORING / MONITORING AGENCY NAME(S) AND ADDRESS(ES)

10. SPONSOR/MONITOR'S ACRONYM(S)

AFRL/RVBXS

11. SPONSOR/MONITOR'S REPORT NUMBER(S)

12. DISTRIBUTION / AVAILABILITY STATEMENT

Approved for public release; distribution is unlimited. (66ABW-2010-1446 dtd 2 Dec 2010)

13. SUPPLEMENTARY NOTES

5th International Conference of Numerical Modeling of Space Plasma Flows (ASTRONUM 2010), Vol 444, 13-18 June 2010. Government Purpose Rights

[1]AFRL/Space Vehicles Directorate, Kirtland AFB, NM, USA; [2]Los Alamos National Laboratory, Los Alamos, NM, USA; [3]National Solar Observatory, Tucson, Arizona, USA

14. ABSTRACT

Global estimates of the solar photospheric magnetic field distribution are critical for space weather forecasting. These global maps are the essential data input for accurate modeling of the corona and solar wind, which is vital for gaining the basic understanding necessary to improve space weather forecasting models. We are now testing the global photospheric field maps generated by the Air Force Data Assimilative Photospheric flux Transport (ADAPT) model as input to the Wang-Sheeley-Arge (WSA) coronal and solar wind model. ADAPT incorporates data assimilation within a modified version of the Worden & Harvey photospheric magnetic flux transport model to provide an instantaneous snapshot of the global photospheric field distribution compared to that of traditional synoptic maps. In this paper we provide an overview of the WSA and ADAPT models, plus discuss preliminary results obtained from WSA when using a traditional versus an ADAPT photospheric field synoptic map as its input.

15. SUBJECT TERMS
Forecasting, CME, Solar Flare

16. SECURITY CLASSIFICATION OF:			17. LIMITATION OF ABSTRACT	18. NUMBER OF PAGES	19a. NAME OF RESPONSIBLE PERSON
a. REPORT	b. ABSTRACT	c. THIS PAGE			Donald Norquist
Unclassified	Unclassified	Unclassified	Unlimited	10	19b. TELEPHONE NUMBER *(include area code)*

Volume Title
ASP Conference Series, Vol. **Volume Number**
Author

Improving Data Drivers for Coronal and Solar Wind Models

C. Nick Arge[1], Carl J. Henney[1], Josef Koller[2], W. Alex Toussaint[3], John W. Harvey[3], and Shawn Young[1]

[1]*AFRL/Space Vehicles Directorate, Kirtland AFB, NM, USA*
[2]*Los Alamos National Laboratory, Los Alamos, NM, USA*
[3]*National Solar Observatory, Tucson, Arizona, USA*

Abstract. Global estimates of the solar photospheric magnetic field distribution are critical for space weather forecasting. These global maps are the essential data input for accurate modeling of the corona and solar wind, which is vital for gaining the basic understanding necessary to improve space weather forecasting models. We are now testing the global photospheric field maps generated by the Air Force Data Assimilative Photospheric flux Transport (ADAPT) model as input to the Wang-Sheeley-Arge (WSA) coronal and solar wind model. ADAPT incorporates data assimilation within a modified version of the Worden & Harvey photospheric magnetic flux transport model to provide an instantaneous snapshot of the global photospheric field distribution compared to that of traditional synoptic maps. In this paper we provide an overview of the WSA and ADAPT models, plus discuss preliminary results obtained from WSA when using a traditional versus an ADAPT photospheric field synoptic map as its input.

1. Introduction

Solar magnetic fields associated with coronal holes that extend into interplanetary space play a key role in the dynamics of the heliosphere. Coronal hole magnetic fields significantly influence the structure of the solar corona and solar wind dynamics. Since the coronal magnetic field is not readily observable, models are required to estimate the magnetic field configuration of the corona, and by extension, the solar wind. Global maps of the observed photospheric magnetic field distribution serve as the primary input to these models. The WSA model (Arge et al. 2004) is an example of such a model. WSA's coronal component can readily determine the 3D structure of the magnetic field, while its solar wind component can provide the speed and the interplanetary magnetic field polarity of the wind at any location in the inner heliosphere. It has become abundantly clear that coronal models are highly sensitive to the large number of problems (e.g., residual monopoles) and uncertainties (e.g., at the poles) in the global maps used to drive them (e.g., Arge & Pizzo 2000; Riley et al. 2006; Hoeksema et al. 1983). Improving the accuracy of these maps is thus essential for reliable modeling of the state of the corona, heliosphere and by extension, the solar wind-magnetosphere interaction. While WSA is simpler than the more advanced 3D MHD models (e.g., MAS and BATS-R-US), it is sensitive to all the problems and uncertainties found in the magnetic field data that advanced models are prone to. This along with the fact that WSA runs quickly and gives results very similar to those obtained from more sophisticated models (e.g., Neugebauer et al. 1998; Riley et al. 2006) makes it ideally suited for testing new and

improved driver data such as that provided by the ADAPT model (Arge et al. 2010). In the following sections we review the WSA and ADAPT models. Additionally, preliminary differences between coronal parameters obtained from WSA based on traditional Carrington and ADAPT map data input are discussed.

2. The WSA Model

The Wang-Sheeley-Arge (WSA) model is a combined empirical and physics based model of the corona and solar wind (Arge & Pizzo 2000; Arge et al. 2003, 2004). It is an improved version of the original Wang and Sheeley model (Wang & Sheeley 1992, 1995). WSA uses ground-based line-of-sight observations of the Sun's surface magnetic field as its input. The photospheric field map is then used in a magnetostatic potential field source surface (PFSS) model (Schatten, Wilcox, & Ness 1969; Altschuler & Newkirk 1969; Wang & Sheeley 1992), which determines the coronal field out to 2.5 solar radii (R_s). The output of the PFSS model serves as input to the Schatten Current Sheet (SCS) model (Schatten 1971), which provides a more realistic magnetic field topology of the upper corona. Only the innermost portion (i.e., from 2.5 R_s to between 5 and 30 R_s) of the SCS solution is used. An empirical velocity relationship (e.g., Arge et al. 2003, 2004) is then used to assign solar wind speed at the chosen outer boundary positioned between 5-30 R_s. It is a function of two coronal parameters: (1) flux tube expansion factor (f_s), and (2) the minimum angular separation at the photosphere between an open field footpoint and the nearest coronal hole boundary. These parameters are determined by starting at the centers of each of the grid cells on the outer coronal boundary surface and tracing the magnetic field lines down to their footpoints rooted in the photosphere. The flux tube expansion factors are calculated using the traditional definition $f_s = (R_{ph}/R_{ss})^2[B_{ph}/B_{ss}]$ (e.g., Wang & Sheeley 1992), where B_{ph} and B_{ss} are the field strengths, along each flux tube, at the photosphere ($R_{ph} = 1R_s$) and the source surface($R_{ss} = 2.5R_s$), respectively. The model provides the radial magnetic field and solar wind speed at the outer coronal boundary surface and these values are then fed into a solar wind model such as the simple WSA 1-D modified kinematic solar wind model (Arge et al. 2004) or even advanced 3-D MHD model solar wind propagation models such as Enlil (e.g., Odstrcil et al. 2004) or LFM-helio (e.g., Pahud et al. 2009).

3. Global Solar Photospheric Magnetic Maps

To date the solar magnetic field has only been recorded for approximately half of the solar surface at any given time. Since the rotation period of the Sun as observed from the Earth is approximately 27 days, any global (or synoptic) map of the solar magnetic field includes data more than 13 days old. These global maps are typically constructed by remapping full-disk magnetograms into heliographic coordinates defined by a fixed rotation rate, typically 27.2753 days (commonly referred to as Carrington synoptic maps). One of the key drawbacks of these maps is that space and time are mixed, since any element of longitude represents the averaging of many magnetograms for periods up to 10 days with no correction of, e.g., differential rotation.

The goal of solar magnetic flux transport models is to provide an estimate of the instantaneous global spatial distribution of the solar magnetic field. These models strive to evolve the synoptic map magnetic flux by incorporating rotational, meridional,

and supergranular diffusive transport processes when and where measurements are not available (e.g., Worden & Harvey 2000; Schrijver & DeRosa 2003, and references therein). Including flux transport aids to minimize potential non-physical monopole moments that periodically occur in Carrington synoptic maps near the solar eastern limb edge of newly merged observed data, and especially during periods when the solar polar regions are not well observed from the Earth.

3.1. Magnetic Flux Transport with ADAPT

The magnetic flux transport model used with ADAPT is a modified version of the Worden and Harvey (WH) model (Worden & Harvey 2000). To date, flux transport, as well as traditional Carrington maps, assimilate new data by simply inserting or blending directly with the evolving model. These blending methods make simplifying assumptions about the accuracy of the data and model. The ADAPT flux transport model, however, incorporates various assimilation methods within the Los Alamos National Laboratory (LANL) data assimilation framework. ADAPT has the option to use either an ensemble least squares (EnLS) estimation (Bouttier & Courtier 2002) or Kalman filter (Evensen 2003) technique. The initial implementation and testing of the Kalman filter proved to be challenging with the bipole nature of solar magnetic data. So, while finalizing the Kalman filter code, the current implementation of ADAPT uses the EnLS method:

$$X_a = X_f + \omega(y - \mathbf{H}(X_f))$$

where X_a, X_f, ω, and y represent the analysis, model forecast (background), weight, and observation values, respectively. The observation operator, **H**, is 1 for observation pixels otherwise zero. The weight, ω, is defined as $\omega = {\sigma_f}^2/({\sigma_f}^2 + {\sigma_y}^2)$, where ${\sigma_f}^2$ and ${\sigma_y}^2$ are the variances of the model ensemble and observed data, respectively.

The WH flux transport model and the LANL data assimilation codes are now fully integrated after significant effort (Arge et al. 2010). The modified WH version allows for the hemispheric differential rotation and meridional flow model parameters to be decoupled. In addition, the modified WH model within ADAPT includes an ensemble of model realizations using different model parameters constrained by the estimated errors of each parameter (e.g., such as meridional drift). The model ensemble is beneficial in two significant ways. First, the ensemble variance is utilized to estimate the model error required by the LANL data assimilation framework. Second, comparing the different ensemble members individually with observations (e.g., solar polar field observations and coronal holes) will provide feedback to determine the magnitude and time dependent behavior of large scale magnetic flow patterns such as the meridional drift rates in each hemisphere.

Additional modifications to the WH model include, for example, how supergranular diffusion is modeled. For sub-daily cadence, the previous WH supergranular diffusion method behavior resulted in flow patterns that had the potential to change abruptly. The new method utilizes continuously varying pixel values initialized randomly from a normal distribution with mean 0 and variance 1. The values are perturbed smoothly within this range for small time steps up to the maximum time step (i.e., the selected mean supergranule lifetime). Though there is not enough space here to adequately explain how the values are scaled (this will be detailed in a subsequent paper), the new method results in a slowly changing flow pattern.

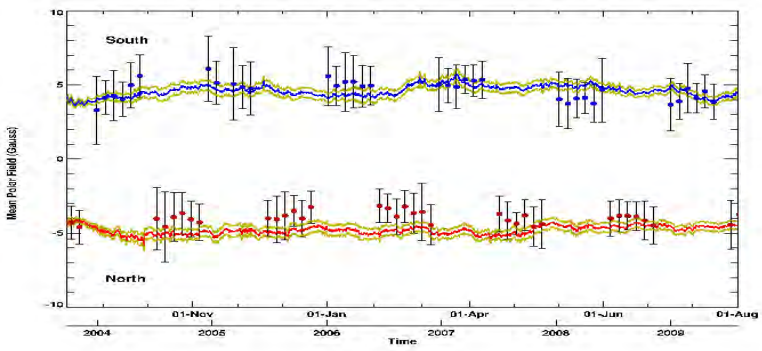

Figure 1. Preliminary comparison between the observed mean polar magnetic field values from MWO magnetograms (dots) with 1-sigma error bars and ADAPT (lines) mean ensemble values. The blue (upper) and red (lower) dots and lines are from the south and north polar bands respectively. The upper and lower yellow lines illustrate the 1-sigma model error for the mean values determined from the ensemble.

4. Polar Fields: Preliminary Validation of ADAPT

One key metric for model parameter feedback is the evolution of the polar magnetic field. Measurements of the line-of-sight field near the Sun's poles are often highly unreliable because of their close proximity to the limb and because the Sun's rotation axis is inclined 7.25° to the ecliptic plane. Field measurements at the solar limb are difficult because only a small component of the field vector is directed toward the observer. This is further complicated by the highly variable horizontal magnetic field signal that becomes increasingly prevalent near the limb (Harvey et al. 2007). In addition, the observed tilt of the Sun from Earth has the effect of rendering one of the poles unobservable for months at a time. Unfortunately, coronal models are exceptionally sensitive to the data located at the solar poles (Arge & Pizzo 2000).

Models such as ADAPT overcome this problem by incorporating key transport processes (i.e., meridional drift and supergranular diffusion) that fill the poles naturally with magnetic flux from lower latitudes. Since the polar fields change slowly over time, ADAPT has the real potential to realistically model the time dependent flux distribution at the poles. Figure 1 shows a preliminary comparison between Mount Wilson Solar Observatory (MWO) measurements of the polar fields when they are well observed (dots with associated error bars) and the field values at the poles as determined by ADAPT (solid lines). This very preliminary result (e.g., using a fixed meridional flow rate for both hemispheres) is very encouraging and demonstrates that model can remain consistent with observations for extended periods of time. In the near term, we plan to use various metrics (e.g., polar field strength and coronal hole boundaries compared with observations during the past 3 to 6 months) to select the best model parameters for each hemisphere.

5. Preliminary WSA results using ADAPT Maps

WSA results are compared using global magnetic maps from ADAPT and standard Carrington as input. As shown in Figure 2, the photospheric field distribution seen in the two input maps (middle left and right plots) are significantly different from one another. In comparing the standard photospheric field Carrington map on the left with the corresponding ADAPT map on the right, it is evident that they differ more and more as one moves toward their right-hand edges. The maps are similar on their left sides because this is where the data have been recently merged into both the maps. The right side of the maps is located on the far-side of the Sun where no new traditional magnetogram data are available. The two maps differ so significantly here because the ADAPT model has evolved the fields using the WH flux transport process, while this is not done in standard Carrington maps and the fields are as they were when they crossed central meridian several days in the past.

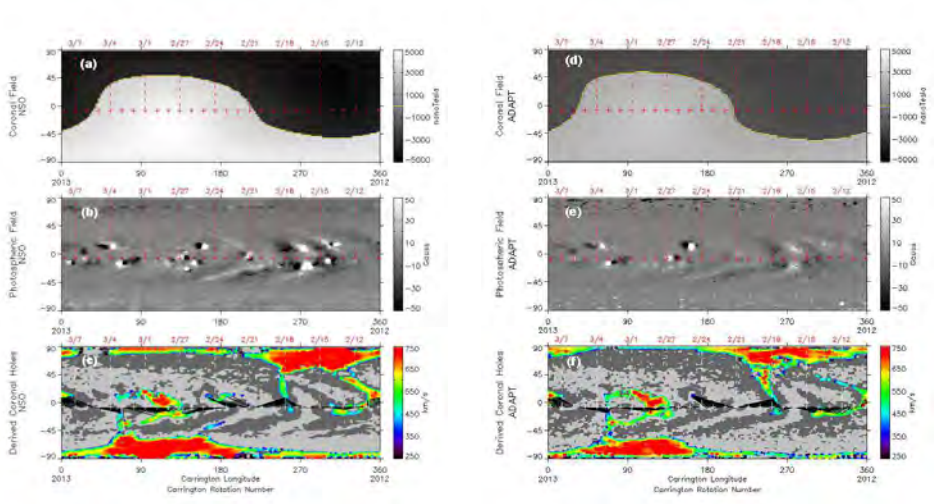

Figure 2. (a & d) Global coronal field polarity at 5 R_s from the WSA model using a National Solar Observatory (NSO) Carrington map (b) and an ADAPT map (e) as input. Outward (Inward) directed field indicted by white (black) areas. The red (or white in c & f) plus signs near the equator mark the daily positions of the sub-earth point. (c & f) Coronal holes as determined by the WSA model. The field polarity at the photosphere is indicated by the light/dark (positive/negative) gray contours, while the colored dots identify the foot-points of the open field lines at the photosphere. The dot color indicates the solar wind speed at 5.0 R_s as predicted by the model. The black straight lines identify the connectivity between the outer (open) boundary located at 5.0 R_s and the source regions of the solar wind at the photosphere (1.0 R_s).

The maps seen at the top of Figure 2 are the radial magnetic field on a spherical surface positioned high (5 R_s) in the corona as determined by the WSA model. There are only subtle morphology differences between the two maps, but the field tends to simplify significantly high up in the corona. The bottom images in Figure 2 show the coronal holes (colored dots) as predicted by the WSA model. Substantial differences are evident in the sizes, shapes, and positions of the open field regions (coronal holes) even on the left side of the maps where the input maps to the model are most similar.

Coronal holes are major sources of the solar wind and these results clearly demonstrate that traditional Carrington maps do not produce the same coronal structure as that obtained using a more realistic, instantaneous snapshot of the global photospheric field distribution.

6. Summary

In this paper, we reviewed the WSA model and the magnetic field maps traditionally used to drive it, plus introduced photospheric flux transport models and the newly developed ADAPT model. Coronal output from WSA using ADAPT generate maps as its input was compared to that obtained from a traditional Carrington map. The preliminary results reveal substantial differences in the sizes, shapes, and positions of the model derived coronal holes when using the two different types of input maps and suggest that traditional Carrington maps do not produce the same coronal structure as that obtained using a more realistic, instantaneous snapshot of the global photospheric field distribution. We also showed that the ADAPT model has the capacity to reproduce the observed polar fields over extended periods of time. Now that ADAPT is working as input to WSA, we plan to do a more thorough validation of the model. For instance, we plan to compare WSA model output with EUVI STEREO observations.

Acknowledgments. This work is supported by a grant from the Air Force Office of Scientific Research (AFOSR) and by the AFRL Space Weather Forecasting Laboratory (SWFL). The NSO data used for this work are produced cooperatively by NSF/NSO. The MWO magnetogram data was provided by R. Ulrich and the staff at MWO.

References

Altschuler, M. A., & Newkirk Jr., G. 1969, Solar Phys., 9, 131
Arge, C. N., Henney, C. J., Koller, J., Compeau, C. R., Young, S., MacKenzie, D., Fay, A., & Harvey, J. W. 2010, Twelfth International Solar Wind Conference, 1216, 343
Arge, C. N., Luhmann, J. G., Odstrcil, D., Schrijver, C. J., & Li, Y. 2004, JASTP, 66, 1295
Arge, C. N., Odstrcil, D., Pizzo, V. J., & Mayer, L. R. 2003, Solar Wind Ten, 679, 190
Arge, C. N., & Pizzo, V. J. 2000, J. Geophys. Res., 105, 10465
Bouttier, F., & Courtier, P. 2002, in Meteorological Training Course Lecture Series, ECMWF, 1
Evensen, G. 2003, Ocean dynamics, 53 (4), 343, DOI:10.1007/s10236-003-0036-9
Harvey, J., Branston, D., Henney, C. J., & Keller, C. U. 2007, ApJ, 659, L177
Hoeksema, J. T., Wilcox, J. M., & Scherrer, P. H. 1983, J. Geophys. Res., 87, 10331
Neugebauer M., Forsyth, R. J., Galvin, A. B., Harvey, K. L., Hoeksema, J. T., Lazarus, A. J., Lepping, R. P., Linker, J. A., Mikić, Z., Steinberg, J. T., von Steiger, R., Wang, Y.-M, & Wimmer-Schweingruber, R. F. 1998, J. Geophys. Res., 103, 14, 587
Odstrcil, D., Riley, P., & Zhao, X. P. 2004, J. Geophys. Res., 109, 2116
Pahud, D. M., Merkin, V. G., Hughes, W., Lyon, J., & McGregor, S. L. 2009, AGU Fall Meeting Abstracts, 1532
Riley, P., Linker, J. A., Mikić, Z., Lionello, R., Ledvinai, S. A., & Luhmann, J. G. 2006, ApJ, 1510, 653
Schatten, K.H. 1971, Cosmic Electrodynamics 2, 232
Schatten, K.H., Wilcox, J.M., & Ness, N.F. 1969, Solar Phys., 9, 442
Schrijver, C. J., & DeRosa, M. L. 2003, Solar Phys., 212, 165
Wang, Y.-M., & Sheeley Jr., N.R. 1992, ApJ, 392, 310
Wang, Y.-M., & Sheeley Jr., N.R. 1995, ApJ, 447, L143
Worden, J., & Harvey, J. 2000, Solar Phys., 195, 247

DISTRIBUTION LIST

DTIC/OCP
8725 John J. Kingman Rd, Suite 0944
Ft Belvoir, VA 22060-6218 1 cy

AFRL/RVIL
Kirtland AFB, NM 87117-5776 2 cys

Official Record Copy
AFRL/RVBXS/Donald Norquist 1 cy

This page intentionally left blank.